

## QED Effects in Cu-Like Pb Recombination Resonances Near Threshold

E. Lindroth,<sup>1</sup> H. Danared,<sup>2</sup> P. Glans,<sup>1,\*</sup> Z. Pešić,<sup>1</sup> M. Tokman,<sup>1</sup> G. Viktor,<sup>1</sup> and R. Schuch<sup>1</sup>

<sup>1</sup>*Department of Atomic Physics, Stockholm University, Frescativägen 24, SE-104 05 Stockholm, Sweden*

<sup>2</sup>*Manne Siegbahn Laboratory, Stockholm University, Frescativägen 24, SE-104 05 Stockholm, Sweden*

(Received 22 December 2000)

In an electron-ion recombination study with  $\text{Pb}^{53+}$  dielectronic recombination resonances are found for as low as  $\sim 10^{-3}$ – $10^{-4}$  eV relative energy. The resonances have been calculated by relativistic many-body perturbation theory and through comparison with experiment the  $\text{Pb}^{53+}(4p_{1/2}-4s_{1/2})$  energy splitting of  $\sim 118$  eV is determined with an accuracy comparable to the position of the first few resonances, i.e.,  $\sim 10^{-3}$  eV. Such a precision provides a test of QED in a many-body environment at a level which can still not be reached in calculations.

DOI: 10.1103/PhysRevLett.86.5027

PACS numbers: 31.30.Jv, 31.15.Ar, 34.80.Lx

Our knowledge about atomic structure and quantum electrodynamical (QED) corrections to energy levels is almost exclusively obtained through photon spectroscopy. Although it would hardly have been anticipated a few years ago, resonances in collision cross sections provide today an alternative access to highly accurate information on atomic energy levels. We show here that one among the presently most accurate measurements of an energy splitting in a few electron highly charged ion is obtained by recombination with free electrons near the ionization threshold. These measurements provide a test of bound state QED in few electron systems.

A collision between one electron and one ion may result in recombination either through a nonresonant photoemission process (radiative recombination, RR) or through a resonant process where the ion is simultaneously excited. The latter process, dielectronic recombination (DR) is an inverse Auger process where the capture is through a doubly excited autoionizing state which finally decays radiatively to a state below the ionization threshold of the recombined ion. Accurate measurements of recombination resonances can be used for critical tests of calculations in order to improve our understanding of formation of atoms and the binding of their constituents. Knowledge of recombination processes is also important for modeling of astrophysical and fusion plasma.

We present cross sections in the form of rate coefficients for recombination of electrons with  $\text{Pb}^{53+}$  and  $\text{Pb}^{54+}$  which shows features at collision energies of 1 meV and below. For the copperlike  $\text{Pb}^{53+}$  ions, DR resonances can form when the  $4s_{1/2}$  electron is excited to  $4p_{1/2}$  while the closed shell core is unchanged, and the free electron recombines into a high  $n\ell$  state. The energies of the resonances are determined by the differences between the  $4p_{1/2}-4s_{1/2}$  energy splitting and the recombination energy. As the lowest energy resonances seem to appear for extremely low relative energy (the first one around  $10^{-4}$  eV and the second around  $10^{-3}$  eV), the resonance positions are fixed very precisely. This fixes the  $4p_{1/2}-4s_{1/2}$  energy splitting as well since the recombination is into high  $n\ell$  states which can be calculated very accurately. Our deter-

mination of the  $\sim 118$  eV large  $4p_{1/2}-4s_{1/2}$  splitting is within 1 meV, i.e., below 0.001% and thus slightly more precise than the determination of the  $2p_{3/2}-2s_{1/2}$  splitting in Li-like bismuth [1].

A lot of efforts have been invested both experimentally [1,2] and theoretically [3–7] to determine energy levels and other properties in heavy highly charged ions with the purpose to test QED in the presence of a strong nuclear field. Highest precision can often be obtained from measurements on systems with more than one electron [1,2] forcing calculations to tackle the problem of QED in a many-electron environment. One approach treats the many-body part starting from some suitable one-particle potential and use then, e.g., relativistic many-body perturbation theory (RMBPT) to calculate higher order corrections to the electron-electron interaction. Radiative effects appearing only with a QED treatment are then calculated in the same one-particle potential (accounting for the *screening* of the QED effects) and should, as a last step, be systematically corrected for higher order corrections to the electron-electron interaction. Although completion of this last step has generally not been possible, results in good agreement with experiments [3–5,7] have been produced. Approaches which calculate radiative and many-body effects on the same footing have also been presented for two [8] and three [9] electron ions.

The experiment has been performed at the CRYRING storage ring in Stockholm. The highly charged  $^{208}\text{Pb}$  ions from an electron-beam ion source were injected via a radio-frequency quadrupole, into the ring, and accelerated to 4.2 MeV/u. The ions were then cooled using an electron beam of 25 mA, whose transverse temperature ( $kT_{\perp}$ , i.e., from the transversal velocity spread), was reduced to around 1 meV by adiabatic expansion with a factor of 100 [10]. After cooling, where the electron velocity matches the ion velocity, i.e.,  $E_e = (m_e/m_i)E_i$ , a change in the lab energy equal to  $\Delta E_e$  introduces a collision energy in the center of mass of  $E_{\text{cm}} \approx \Delta E^2/4E_e$ . Zigzag scans were made from zero relative velocity (cooling) up to an electron velocity that corresponds to  $E_{\text{cm}} \sim 1$  eV, and then, after crossing zero relative velocity, to electron velocities

smaller than the ion velocity, and finally back to zero relative velocity. In this way four complete spectra were obtained. After applying corrections due to the electron-beam space charge and the drag force, by which the electrons accelerate the ions when velocities are not matched, the four spectra can be added. The alignment of the DR peaks in the four spectra serves as a check on the corrections and on the accuracy of the energy calibration, which is essential for a reliable comparison with theory. Charge-changed ions hit a YAP:Ce (YAlO<sub>3</sub>, Ce-doped perovskite) scintillator detector behind the second ring dipole after the electron cooler. This detector has the necessary advantage of a high irradiation threshold. The rate coefficients are determined by  $\alpha_{\text{exp}} = (\gamma^2 R L_r) / (n_e N_i L_{\text{int}})$ , where  $\gamma$  is the Lorentz factor,  $R$  is the background corrected counting rate of recombined ions,  $N_i$  is the number of ions stored in the ring, and  $L_r$  and  $L_{\text{int}}$  are the lengths of the ring and of the interaction region, respectively. At a vacuum of  $10^{-11}$  Torr, the electron capture background is at most in the percent level of the total detected charge-exchanged particles at  $E_{\text{cm}} = 0$ . The systematic experimental uncertainty is about 15%, where 10% comes from the absolute number of stored ions (determined by a current transformer during injection or destruction of the beam) and 5% from the effective interaction length.

Figure 1 shows the recombination rate as a function of relative energy for Pb<sup>54+</sup> and Pb<sup>53+</sup>. The Pb<sup>54+</sup> spectrum must be dominated by RR since it is smooth and shows

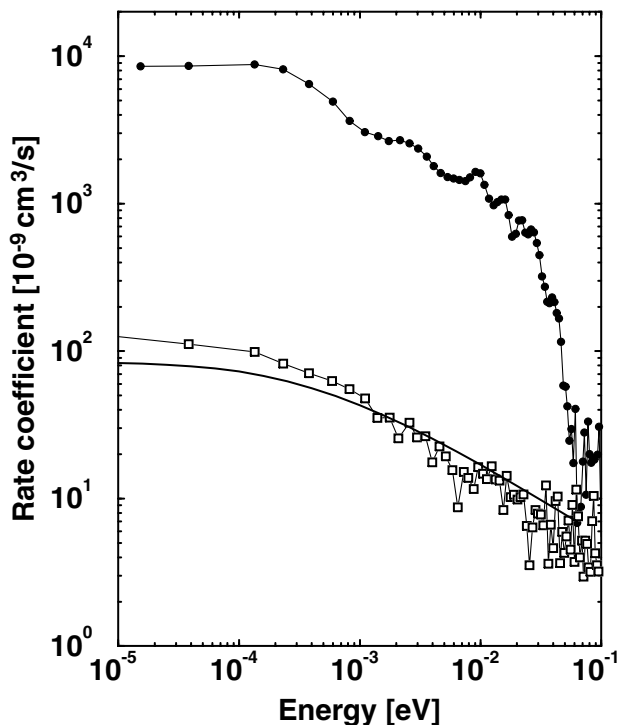
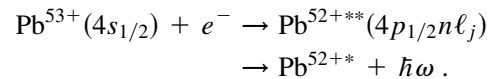


FIG. 1. Measured recombination rate coefficients ( $\alpha_{\text{exp}}$ ) for Pb<sup>53+</sup>, circles, and Pb<sup>54+</sup>, squares, as a function of relative energy. The solid line shows the calculated contribution from radiative recombination for Pb<sup>54+</sup>.

no sign of resonances. The rate for Pb<sup>53+</sup> is in comparison enhanced with nearly 2 orders of magnitude due to dielectronic recombination resonances. Several of these are clearly seen in the spectrum with the lowest one at only  $10^{-4}$  eV. This explains the large difference in beam lifetime for Pb<sup>54+</sup> and Pb<sup>53+</sup> which was first observed at CERN [11]. Similar differences were also found for Au<sup>50+</sup> and Au<sup>49+</sup> [12], where also recombination spectra were recorded. Although enhanced recombination rates have been detected in several storage ring experiments during the last years [13–15] it has never been possible to detect an isolated resonance as close to threshold and to measure such a high recombination rate as here.

DR of Pb<sup>53+</sup> can be regarded as a two-step process:



The intermediate state is the resonant doubly excited state and the final state is any state bound below the ionization threshold. The resonances will appear for electron energies  $\varepsilon_{e^-} = E(4p_{1/2-4s_{1/2}}) + \Delta E$  where  $\Delta E$  is the binding energy of the last electron,  $\Delta E = E(4p_{1/2}n\ell_j) - E(4p_{1/2})$ . If it is possible to calculate  $\Delta E$  very accurately, the  $4p_{1/2-4s_{1/2}}$  splitting can be obtained from the energy positions of the recombination resonances. Table I shows the accuracy with which different contributions to the Pb<sup>53+</sup>( $4p_{1/2-4s_{1/2}}$ ) splitting can be calculated at present. More details can be found in [16,17], where a comparison with an earlier calculation [18] is also made. The method is further described and applied to Li-like systems in, e.g., Refs. [19,20]. The main uncertainty in the RMBPT part of the calculation comes from the extrapolation to include contributions from partial waves with  $\ell \geq 11$  and is conservatively estimated to 1 meV. Higher order correlation is calculated by RMBPT in an all order formulation [19]. Table I lists also radiative contributions from Indelicato [21], evaluated in the nuclear potential (one photon exchange) as well as in a potential describing the closed shell core (screening). The result is an approximation in two ways. First, the one-electron two-photon diagrams are missing; they have hitherto not been fully accounted for in any ion. An estimate of their size in Ref. [6] gave 1 eV for the ground state in hydrogenlike uranium. The effects scale roughly as  $Z^5$  and  $1/n^3$ , pointing to a possible 10 meV contribution to the Pb<sup>53+</sup>( $4s$ ) binding energy. Second, the many-body corrections to the QED contributions are only approximately accounted for. Blundell [3] has earlier found similar screening contributions. In addition he included some of the more complicated many-body corrections (called valence external exchange terms, core QED in Ref. [3]) and found  $\sim -40$  meV contributions to the  $4p_{1/2-4s_{1/2}}$  energy splitting. The 40 meV uncertainty in the radiative contributions given in Table I is thus a rough estimate of possible additional radiative corrections and dominates completely the uncertainty of the  $4p_{1/2-4s_{1/2}}$  energy. The measured spectrum for Pb<sup>53+</sup>

TABLE I. Contributions to the  $4p_{1/2}$ - $4s_{1/2}$  splitting (eV).

	$4p_{1/2}$ - $4s_{1/2}$
Dirac-Fock (including nuclear size effects)	118.570 88
Breit 1st order (including retardation)	1.713 60
Higher order Breit corrections to the Dirac-Fock value <sup>(a)</sup>	-0.055 89
Mass polarization (Dirac-Fock)	-0.004 89
2nd order Coulomb + Breit correlation <sup>(b)</sup>	-0.1736(10)
Higher order Coulomb + Breit correlation <sup>(c)</sup>	0.003 48
Total RMBPT	120.054(1)
Rad. corr. (screened self-energy and vacuum polarization) [21]	-2.008(40)
Sum	118.046(40)
Extracted from the present experiment	118.010(1)

<sup>(a)</sup>Also called Breit-RPA, given in Refs. [16,17] together with the 2nd order correlation.

<sup>(b)</sup> $\ell_{\max} = 10$  and extrapolated from there.

<sup>(c)</sup> $\ell_{\max} = 8$ .

shows a number of resonances between threshold and  $\sim 40$  meV, i.e., within a region of the same size as the uncertainty. Given this uncertainty one has now to identify the resonances. For this we have to calculate  $\Delta E$ , which gives the distribution of the states relative to each other and vary  $E(4p_{1/2}$ - $4s_{1/2})$  within the 40 meV uncertainty to match the measured spectrum as well as possible.

Table I gives the  $4p_{1/2}$ - $4s_{1/2}$  energy splitting to  $\sim 118$  eV. This is close to the binding energy for a  $n = 18$  electron as can be estimated even from the non-relativistic hydrogenlike energy with  $Z_{\text{eff}} = 53$ . A relativistic, but still hydrogenlike, determination of the  $18\ell_j$  states, shows that the doubly excited states due to  $4p_{1/2}18\ell_j$  configurations are spread out both below and above the ionization threshold and only those including the higher  $18\ell_j$  states can form resonances. The distances between the first clearly seen resonances are slightly below 10 meV and decrease for higher energy. This fits well with the distances between the  $18\ell_j$  states starting from  $j = 21/2$ , as is seen in Fig. 2. The data are not compatible with the first resonances being due to configurations with  $18\ell_{19/2}$  or  $18\ell_{23/2}$ . Already at this point the  $4p_{1/2}$ - $4s_{1/2}$  energy splitting is determined within 10 meV, i.e., within the distance to nearby fine structure levels. When the interaction with the core is accounted for, through the Dirac-Fock approximation, the  $18n_{21/2}$  and the  $18o_{21/2}$  ( $\ell = 10$  and  $\ell = 11$ ) states split with 0.4 meV. Additional contributions of 0.1–0.2 meV arise from core polarization, but the energy is still more or less completely decided by the  $j$ -quantum number of the  $n = 18$  electron. This is still the case when the full interaction between the  $18\ell_j$  and the  $4p_{1/2}$  electrons is accounted for. For each  $j$  of the outer electron there are four  $(4p_{1/2}18\ell_j)_J$  states, two of each parity, which spread out over  $\approx 1$  meV, as is seen in Fig. 2. To describe these autoionizing states we use, as earlier [20], a combination of RMBPT and *complex rotation*. The widths vary significantly. Of the states dominated by a certain  $4p_{1/2}18\ell_j$  configuration, one is narrow and one much broader. For  $j = 21/2$  the broad states

have a width of a few meV and the autoionization width of the narrow ones is  $\sim 0.01$  meV. A broad resonance arises when the  $(4p_{1/2}18\ell_j)_J$  state is able to decay to  $(4s_{1/2}\varepsilon_{\ell+1})_J$  which means that no change in direction of the individual angular momenta is needed.

As stated above the identification of the resonances at  $\sim 3$  meV to be due to  $4p_{1/2}18\ell_{21/2}$  doubly excited states fixes the  $4p_{1/2}$ - $4s_{1/2}$  splitting within 10 meV. We have then varied the splitting within a few meV to obtain the best agreement with the measured spectrum. For such a direct comparison the calculated cross section needs to be folded with the electron-beam temperature. Figure 3 shows the result assuming the nominal velocity spread ( $kT_{\perp} = 1$  meV and  $kT_{\parallel} = 0.08$  meV). Misalignment could give a higher  $kT_{\perp}$ , thus 2 meV are also tested, but  $kT_{\perp} = 1$  meV gives a somewhat better agreement. A  $4p_{1/2}$ - $4s_{1/2}$  energy splitting of 118.010(1) eV is found through the comparison. This corresponds to an additional contribution

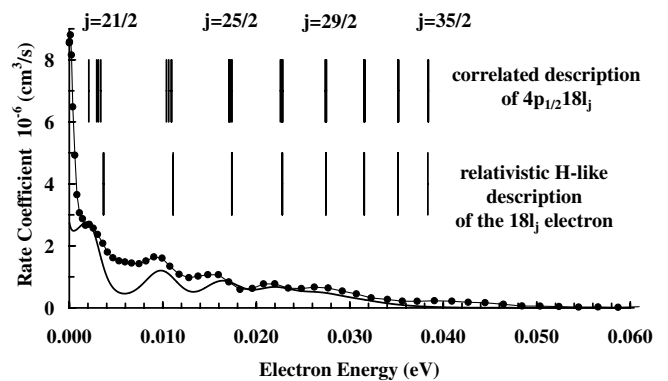


FIG. 2. Calculated rate coefficients, solid line, are shown together with energy positions of the  $4p_{1/2}18\ell_j$  resonances and  $\alpha_{\text{exp}}$ . For each  $j$  of the outer electron there are four  $(4p_{1/2}18\ell_j)_J$  states, two of each parity, spread out over  $\approx 1$  meV. The folding of the calculated cross sections with an electron velocity distribution characterized by  $kT_{\perp} = 1$  meV and  $kT_{\parallel} = 0.08$  meV causes a small peak shift compared to the energies of the resonant states.

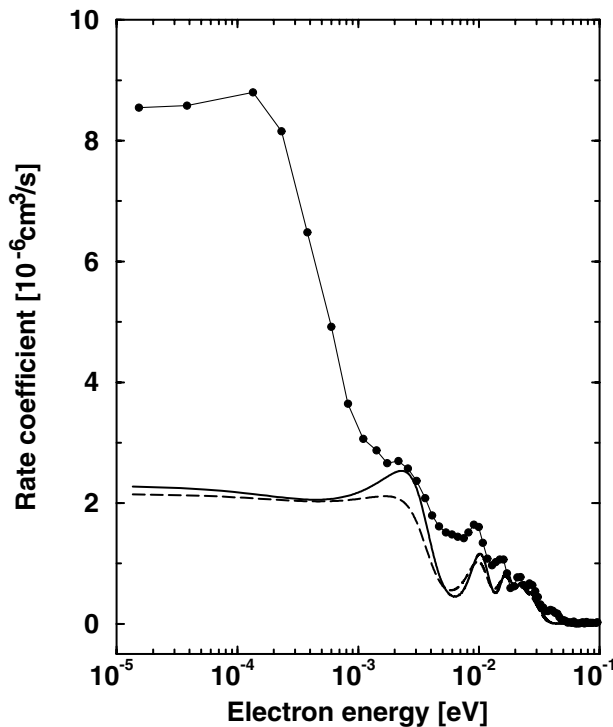


FIG. 3. Recombination rate coefficients for  $\text{Pb}^{53+}$ . The solid and dashed lines show the calculated cross section folded with  $kT_{\perp} = 1$  meV,  $kT_{\parallel} = 0.08$  meV and  $kT_{\perp} = 2$  meV,  $kT_{\parallel} = 0.08$  meV, respectively.

from radiative corrections of  $-0.036(1)$  eV compared to the calculated value in Table I. The radiative contributions should thus be  $-2.044(1)$  eV which is in very good agreement with the value given by Blundell, of  $-2.05(1)$  eV [3].

One might still wonder how certain the identification of the resonances is. If one assigns the  $\sim 3$  meV resonance to  $4p_{1/2}18\ell_{19/2}$  or even to  $4p_{1/2}18\ell_{17/2}$  instead of  $4p_{1/2}18\ell_{21/2}$  one gets an increased intensity around 40 meV where the experiment shows a small hump (Figs. 2 and 3), but the distances between the peaks cannot be reproduced [16]. One possibility is that this small hump is due to some other resonance. We have checked all the other  $4\ell_j n\ell'_j$  series and found no resonances within 1 eV from the threshold. The hump could arise from some isolated resonance, but it cannot be a member of a strong series and should thus not influence the spectrum at lower energies. At the low energy side of the spectrum, see Fig. 3, the calculation shows a flat contribution coming from the broader  $4p_{1/2}18\ell_{21/2}$  resonances while the experiment indicates a resonance slightly below  $2 \times 10^{-4}$  eV. This structure appears even more clearly in the four raw spectra of the zigzag scan [16] and remains, as seen in Fig. 3, after their addition. Independently, the lifetime of  $\text{Pb}^{53+}$  ions in the ring during electron cooling supports the high value of  $\alpha_{\text{exp}}$  at  $E_{\text{cm}} \approx 0$ . One possibility could be that there is a missing resonance. We have tested to add a vanishingly narrow resonance and to fold it with  $kT_{\perp} = 1$  meV and  $kT_{\parallel} = 0.08$  meV. Being that

close to threshold the resonance is, however, smeared out due to the electron-beam energy spread and no maximum  $\sim 2 \times 10^{-4}$  eV could be obtained. If we assume a resonance with a realistic width,  $\sim 10^{-4}$  eV from the  $4p_{1/2}-4s_{1/2}$  radiative rate, we need an enhancement of a factor of 3 to obtain the experimental rate coefficients. This is not far from the enhancement found for RR in  $\text{Pb}^{54+}$  and could thus be interpreted as a similar effect. The structure around  $2 \times 10^{-4}$  eV can, however, not be reproduced with any realistic assumptions for the temperature and the width. One might speculate if there can be special threshold effects not accounted for in the calculation which might produce the peak at  $2 \times 10^{-4}$  eV. This could be a subject of future investigations.

In conclusion, narrow recombination resonances closely above the ionization threshold in highly charged ions allow a determination of energy splittings with presently highest accuracy. This can only be matched by QED calculations with a precision beyond what is possible with methods available today. We have here compared measurement and calculations on DR resonances and extracted the  $4p_{1/2}-4s_{1/2}$  splitting in  $\text{Pb}^{53+}$  with an accuracy of 1 meV, corresponding to a precision of  $8 \times 10^{-6}$ .

P. Indelicato is thanked for communicating results prior to publication. Financial support was received from the Swedish Natural Science Research Council (NFR). M. T. is grateful for support from the Swedish Royal Academy of Science.

\*Present address: Department of Engineering, Physics and Mathematics, Mid-Sweden University, S-851 70 Sundsvall, Sweden.

- [1] P. Beiersdorfer *et al.*, Phys. Rev. Lett. **80**, 3022 (1998).
- [2] J. Schweppe *et al.*, Phys. Rev. Lett. **66**, 1434 (1991).
- [3] S. A. Blundell, Phys. Rev. A **47**, 1790 (1993).
- [4] P. Indelicato and P.J. Mohr, Theor. Chim. Acta **80**, 207 (1991).
- [5] I. Lindgren *et al.*, Phys. Rev. A **47**, R4555 (1993).
- [6] S. Mallampalli and J. Sapirstein, Phys. Rev. A **57**, 1548 (1998).
- [7] K. T. Cheng *et al.*, Phys. Rev. A **62**, 054501 (2000).
- [8] H. Persson *et al.*, Phys. Rev. Lett. **76**, 204 (1996).
- [9] V. A. Yerokhin *et al.*, Phys. Rev. Lett. **85**, 4699 (2000).
- [10] H. Danared *et al.*, Nucl. Instrum. Methods Phys. Res., Sect. A **441**, 123 (2000).
- [11] S. Baird *et al.*, Phys. Lett. B **361**, 184 (1995).
- [12] O. Uwira *et al.*, Hyperfine Interact. **108**, 149 (1997).
- [13] A. Müller *et al.*, Phys. Scr. **T37**, 62 (1991).
- [14] H. Gao *et al.*, Phys. Rev. Lett. **75**, 4381 (1995).
- [15] G. Gwinner *et al.*, Phys. Rev. Lett. **84**, 4822 (2000).
- [16] M. Tokman *et al.*, Phys. Scr. (to be published).
- [17] M. Tokman *et al.*, Hyperfine Interact. (to be published).
- [18] W.R. Johnson *et al.*, Phys. Rev. A **42**, 1087 (1990).
- [19] E. Lindroth and J. Hvarfner, Phys. Rev. A **45**, 2771 (1991).
- [20] W. Zong *et al.*, Phys. Rev. A **56**, 386 (1997).
- [21] P. Indelicato (private communication).